Metadynamics Simulation of Prion Protein: β-Structure Stability and the Early Stages of Misfolding

Alessandro Barducci,[†,‡] Riccardo Chelli,[†,‡,§] Piero Procacci,[†,‡] Vincenzo Schettino,[†,‡] Francesco L. Gervasio,[∥] and Michele Parrinello*,[∥]

Contribution from the Dipartimento di Chimica, Università di Firenze, Via della Lastruccia 3, I-50019 Sesto Fiorentino, Italy, European Laboratory for Nonlinear Spectroscopy (LENS), Via Nello Carrara 1, I-50019 Sesto Fiorentino, Italy, Consorzio Interuniversitario Nazionale per la Scienza e Tecnologia dei Materiali (INSTM), Firenze, Italy, and Computational Science, Department of Chemistry and Applied Biosciences, ETH Zurich, USI Campus, Via Giuseppe Buffi 13, CH-6900 Lugano, Switzerland

Received October 18, 2005; E-mail: parrinello@phys.chem.ethz.ch

Abstract: In the present study we have used molecular dynamics simulations to study the stability of the antiparallel β-sheet in cellular mouse prion protein (PrP^C) and in the D178N mutant. In particular, using the recently developed non-Markovian *metadynamics* method, we have evaluated the free energy as a function of a reaction coordinate related to the β-sheet disruption/growth. We found that the antiparallel β-sheet is significantly weaker in the pathogenic D178N mutant than in the wild-type PrP^C. The destabilization of PrP^C β-structure in the D178N mutant is correlated to the weakening of the hydrogen bonding network involving the mutated residue, Arg164 and Tyr128 side chains. This in turn indicates that such a network apparently provides a safety mechanism for the unzipping of the antiparallel β-sheet in the PrP^C. We conclude that the antiparallel β-sheet is likely to undergo disruption rather than growth under pathogenic conditions, in agreement with recent models of the misfolded monomer that assume a parallel β-helix.

1. Introduction

The prion protein (PrP) is a GPI-anchored surface glycoprotein which has been linked to a vast class of neurodegenerative diseases known as transmissible spongiform encephalopathies. These disorders are caused by a partial unfolding of the normal cellular prion protein (PrP^C) and its conversion to an aberrant, oligomeric form (PrP^{Sc}) which tends to aggregate in amyloid plaques. The structure of PrP^C has been determined by NMR spectroscopy for many species, and it consists of a flexible N-terminal region and a globular domain in the C-terminal region. This domain (124−231 in mouse numbering) is made up of three α-helices and a short antiparallel β-sheet (see Figure 1). The insolubility of PrP^{Sc} has prevented the use of X-ray diffraction and NMR spectroscopy to determine its structure, and a high-resolution structure for PrP^{Sc} monomer is still unavailable. Earlier spectroscopic studies indicated that during conversion to the misfolded isoform a major shift occurs in its secondary structure, with a relevant increase of β-structure involving nearly 50% of the 124−231 chain.[1] Recent electron microscopy data on bidimensional crystals of infectious prion aggregates showed evidence of a PrP^{Sc} trimeric assembly and
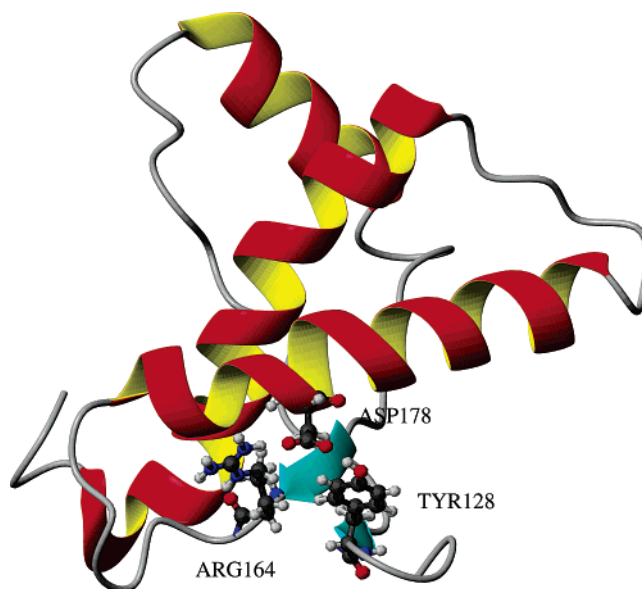

Figure 1. Structure of the mouse PrP^C globular domain (124−226). The Arg164, Tyr128, and Asp178 residues are highlighted.

provided some structural constraints for the PrP^{Sc} monomer structure.[2]

Further experimental input comes from threading experiments[3] and Raman optical activity[4] measurements. Two con-

† Università di Firenze.
‡ European Laboratory for Nonlinear Spectroscopy (LENS).
§ Consorzio Interuniversitario Nazionale per la Scienza e Tecnologia dei Materiali (INSTM).
∥ ETH Zurich.

(1) Pan, K.; Baldwin, M.; Nguyen, J.; Gasset, M.; Serban, A.; Groth, D.; Mehlhorn, I.; Huang, Z.; Fletterick, R. J.; Cohen, F. E.; Prusiner, S. B. *Proc. Natl. Acad. Sci. U.S.A.* **1993**, *90*, 10962−10966.

(2) Wille, H.; Michelitsch, M. D.; Génebaut, V.; Supattapone, S.; Serban, A.; Cohen, F. E.; Agard, D. A.; Prusiner, S. B. *Proc. Natl. Acad. Sci. U.S.A.* **2002**, *99*, 3563−3568.

trasting structural models of PrP^{Sc} have been suggested. In the older model the structure is characterized by two α-helices and a large multistranded antiparallel β-sheet which grows on the shorter pre-existing β-sheet of the noninfectious PrP^C.[5−7] In the newer model, PrP^{Sc} has instead a left-handed parallel β-helix structure. This would be consistent with the increasing experimental evidence that amyloid fibrils adopt parallel β-structures.[3,8,9]

Due to the very high free energy barriers, the conformational transition PrP^C → PrP^{Sc} takes place on a very long time scale and the disease incubation time for humans is a matter of years. However either point mutations or appropriate physicochemical conditions can strongly accelerate misfolding.[10−12] Therefore, such "pathogenic perturbations" have been implemented in molecular dynamics (MD) simulations in order to monitor changes or reveal local instabilities in the PrP^C tertiary structure that could give insight into the conformational transition.[6,7,13−17] In particular, a great deal of attention has been focused on the stability of the small antiparallel β-sheet in pathogenic mutants and/or in pathogenic conditions.[6,7,17,18] Indeed, given the two putative and alternative models for PrP^{Sc}, two possible scenarios can occur. On one hand the antiparallel β-sheet in PrP^C must break down at some stage of the conversion if part of the PrP chain has to evolve toward a parallel β-helix. On the other hand the antiparallel β-sheet should strengthen if the PrP^{Sc} β-structure is built up on this structural element. In this respect, in two recent MD studies[6,7] on the Syrian hamster PrP at low pH, significant structural changes involving the growth of the antiparallel β-sheet were predicted, thereby supporting the hypothesis of the antiparallel β-strand addition as the preferential pathway for the conformational conversion to PrP^{Sc}. Although an antiparallel β-structure could in principle rationalize the electronic microscopy data,[7] there exist, as stated above, several experimental indications[3,8,9] that support the opposite hypothesis, i.e., the occurrence of a PrP^{Sc} parallel β-fold.

However it must be stressed that, even under strongly pathogenic conditions, the conformational barriers remain high and studying these transitions by MD simulations is very challenging. For instance in the huPrP D178N mutant Sekijima et al.[16] found a slight weakening of the β-motif with respect to the wild-type (WT), while Gsponer et al. concluded that "the D178N mutant did not deviate from the NMR conformation more than the wild-type in the nanosecond time scale of the simulation".[13] As stated above, in an acid environment the WT was reported to exhibit a massive β-sheet buildup by Alonso et al.[6] and DeMarco et al.,[7] while Sekijima et al.[16] reported only a moderate strengthening. Also in the connected problem of the neighboring helix 1 stability, different conclusions have been reached.[6,7,19]

In this paper we focus on the stability of the mouse PrP^C antiparallel β-sheet in the WT and in its D178N mutant in water solution. This mutation is universally believed to be infectious and to weaken the structure in a key position. In fact Asp178 anchors the two β-strands and the bracketed helix 1 to the protein core via the salt bridge Asp178-Arg164 and the hydrogen bond (H-bond) between Asp178 and Tyr128 side chains (see Figure 1). The structural relevance of Asp178 has been confirmed by urea-induced unfolding studies.[20] Furthermore, the D178N point mutation has been experimentally found to remarkably and specifically enhance PrP^C conversion to PrP^{Sc}-like isoforms when PrP^C is expressed in the cytosol.[11] Moreover in an acid environment where Asp178 is expected to be protonated and hence unable to bind effectively Arg164 and Tyr128 side chains as in the D178N mutant, PrP^{Sc}-like aggregates are spontaneously formed. Thus a comparative study of WT and D178N mutant can provide important clues to the initial step of PrP^C → PrP^{Sc} transition and PrP^{Sc} structure. To this end we used a recently developed non-Markovian sampling methodology (*metadynamics*).[21] This technique, at variance with standard MD simulations and other sampling methodologies, has proved its ability to overcome very large barriers, thereby providing the free energy profiles in a vast class of complex molecular systems.[22−24] For example, in ref 22 Gervasio et al. have shown that in the docking of β-trypsin with benzamidine in water solution the metadynamics is at least 1 order of magnitude faster than the weighted histogram Umbrella Sampling method.[25] The free energy profiles calculated in the present study clearly indicate that an antiparallel β-structure is significantly weaker in the pathogenic D178N mutant than in WT PrP^C. The destabilization of the PrP^C structure in this region is found to be strongly correlated to the weakening of the H-bond network, involving the mutated residue, Arg164 and Tyr128, caused by the replacement of Asp178 by an Asn residue. Our results, in agreement with the conclusions of refs 2 and 3, strongly indicate that the antiparallel β-sheet is likely to undergo disruption rather than growth in the initial stage of the conversion to the pathogenic form, in contrast with ref 5 and the more recent refs 6 and 7.

2. Methods

The Amber03 force field[26] was adopted. The temperature of the system was set to 300 K, and the pressure, to 0.1 MPa. The technical details of the MD protocol concerning the system composition, the

(3) Govaerts, C.; H.Wille,; Prusiner, S. B.; Cohen, F. E. *Proc. Natl. Acad. Sci. U.S.A.* **2004**, *101*, 8342−8347.

(4) McColl, I. H.; Blanch, E. W.; Gill, A. C.; Rhie, A. G. O.; Ritchie, M. A.; Hecht, L.; Nielsen, K.; Barron, L. D. *J. Am. Chem. Soc.* **2003**, *125*, 10019−10026.

(5) Huang, Z.; Prusiner, S. B.; Cohen, F. E. *Folding Des.* **1996**, *1*, 13−19.

(6) Alonso, D. O.; DeArmond, S. J.; Cohen, F. E.; Daggett, V. *Proc. Natl. Acad. Sci. U.S.A.* **2001**, *98*, 2985−2989.

(7) DeMarco, M. L.; Daggett, V. *Proc. Natl. Acad. Sci. U.S.A.* **2004**, *101*, 2293−2298.

(8) Petkova, A. T.; Ishii, Y.; Balbach, J. J.; Antzutkin, O. N.; Leapman, R. D.; Delaglio, F.; Tycko, R. *Proc. Natl. Acad. Sci. U.S.A.* **2002**, *99*, 16742−16747.

(9) Der-Sarkissian, A.; Jao, C. C.; Chen, J.; Langen, R. *J. Biol. Chem.* **2003**, *278*, 37530−37535.

(10) Prusiner, S. B. *Trends Biochem. Sci.* **1996**, *21*, 482−487.

(11) Ma, J.; Lindquist, S. *Science* **2002**, *298*, 1785−1788.

(12) Riesner, D. *Br. Med. Bull.* **2003**, *66*, 21−33.

(13) Gsponer, J.; Ferrara, P.; Caflisch, A. *J. Mol. Graphics Modell.* **2001**, *20*, 169−182.

(14) El Bastawissy, E.; Knaggs, M. H.; Gilbert, I. H. *J. Mol. Graphics Modell.* **2001**, *20*, 145−154.

(15) Gu, W.; Wang, T.; Zhu, J.; Shi, Y.; Liu, H. *Biophys. Chem.* **2003**, *104*, 79−94.

(16) Sekijima, M.; Motono, C.; Yamasaki, S.; Kaneko, K.; Akiyama, Y. *Biophys. J.* **2003**, *85*, 1176−1185.

(17) Barducci, A.; Chelli, R.; Procacci, P.; Schettino, V. *Biophys. J.* **2005**, *88*, 1334−1343.

(18) Guilbert, C.; Ricard, F.; Smith, J. C. *Biopolymers* **2000**, *54*, 406−415.

(19) Dima, R. I.; Thirumalai, D. *Proc. Natl. Acad. Sci. U.S.A.* **2004**, *101*, 15335−15340.

(20) Liemann, S.; Glockshuber, R. *Biochemistry* **1999**, *38*, 3258−3267.

(21) Laio, A.; Parrinello, M. *Proc. Natl. Acad. Sci. U.S.A.* **2002**, *99*, 12562−12566.

(22) Gervasio, F. L.; Laio, A.; Parrinello, M. *J. Am. Chem. Soc.* **2005**, *127*, 2600−2607.

(23) Ceccarelli, M.; Danelon, C.; Laio, A.; Parrinello, M. *Biophys. J.* **2004**, *87*, 58−64.

(24) Gervasio, F. L.; Laio, A.; Iannuzzi, M.; Parrinello, M. *Chem.−Eur. J.* **2004**, *10*, 4846−4852.

(25) Patey, G. N.; Chandrasekhar, J. P. V.; Madura, J. D.; Impey, R. W.; Klein, M. L. *J. Chem. Phys.* **1975**, *63*, 2334−2339.

integration method, the thermodynamic ensemble, the electrostatic interaction treatment, and the thermalization procedure are given in ref 17. In ref 17 it was shown, by monitoring the root-mean-square displacements of the α-carbons, that the thermalization procedure leads to an equilibrated structure both in the WT and in the D178N mutant. All calculations were performed with the program ORAC.[27] In light of previous experiences,[17] particular care was devoted to the sampling protocol. In this respect we use here the recently introduced metadynamics.[21] This technique consists essentially of a modification of a standard MD simulation in which harmonic restraints are imposed on appropriately selected collective coordinates of the system along with a history-dependent potential. The time-dependent restraint is evolved using the extended Lagrangian method.[28] The history-dependent potential, by summing up Gaussian functions at regular time intervals along the trajectory of the auxiliary variables, disfavors configurations in the space of the real reaction coordinates that have already been visited, while at the same time reconstructing the negative of free energy surface (FES) as a function of the reaction coordinates. The metadynamics method is discussed in more detail in ref 28. In the present case our objective is to assess the relative thermodynamic stability of the antiparallel β-sheet (129−131,161−163) in the WT PrP^C and in its D178N mutant. To this aim we have defined the following collective reaction coordinate

$$S = \sum_{i=1}^{N_{hb}} \frac{1 - (r_i/2.5)^6}{1 - (r_i/2.5)^{12}} \tag{1}$$

where the sum is extended to the four H-bonds of the PrP^C antiparallel β-sheet (129−131,161−163), and r_i is the length of the *i*th H-bond. S approaches 4 when all H-bonds are in place and is equal to zero when the two β-strands are completely detached. By running the metadynamics along such a coordinate, we reconstruct the FES as a function of the length of the β-sheet. When $S = 0$ the β-sheet is severed and the system explores a very large conformational space with many deep minima. In this region S alone is not able to describe the system properly and should be supplemented with other variables. On the other hand this region of configurational space is of little interest for the problem studied here. Therefore, we introduced a reflecting potential wall at $S = 0.1$ the purpose of which is to limit S to values physically relevant for the problem at hand. In the explored S range, the system experiences quite limited structural perturbations (see also section 3). For example, during a metadynamics simulation of the WT PrP^C, the difference between the maximum and minimum distance of the α-carbons of residues belonging to the two β-strands (Leu130 and Tyr162) is about 3 Å. Similar values have been found for the other simulations. However we still noticed a small effect on the FES due to transverse collective motions. For this reason we performed, for each of the two systems (WT and D178N mutant), six independent metadynamics runs of 1.8 ns for a total length of 21.6 ns and averaged the FESs out as follows. We have evaluated the FES for each run, taking the point $S = 2$ as the zero free energy point. When so aligned, the mean square deviation of the FES, integrated from $S = 0.3$ to $S = 3.7$, was evaluated and then minimized relative to the end point of each trajectory. The end points were chosen in the range 1.2−1.8 ns. In this way we obtained an average FES that is well converged being insensitive to the choice of the zero free energy point in the interval from $S = 1.5$ to $S = 2.5$. The parameters of the metadynamics (see ref 28) are the following: the force constant of the harmonic constraint is 1200 kJ mol^{-1}, the auxiliary
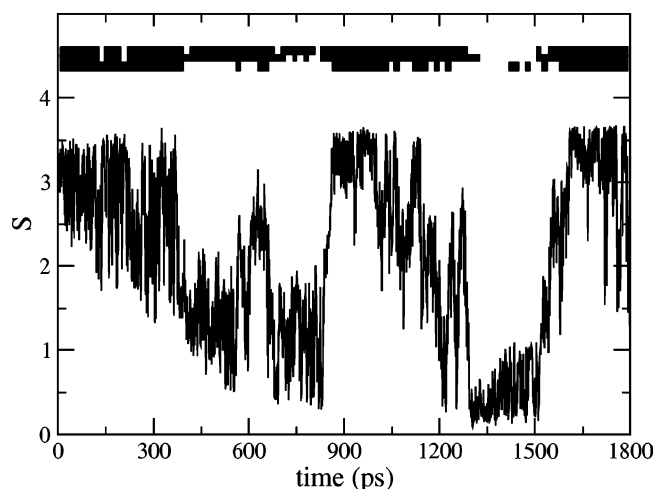
(26) Duan, Y.; Wu, C.; Chowdhury, S.; Lee, M. C.; Xiong, G. M.; Zhang, W.; Yang, R.; Cieplak, P.; Luo, R.; Lee, T.; Caldwell, J.; Wang, J. M.; Kollman, P. *J. Comput. Chem.* **2003**, *24*, 1999−2012.
(27) Procacci, P.; Darden, T. A.; Paci, E.; Marchi, M. *J. Comput. Chem.* **1997**, *18*, 1848−1862.
(28) Laio, A.; Rodriguez-Fortea, A.; Gervasio, F. L.; Ceccarelli, M.; Parrinello, M. *J. Phys. Chem. B* **2005**, *109*, 6714−6721.

Figure 2. Time evolution of S (bottom of the picture) and of the length of the PrP^C β-sheet (top of the picture) calculated by STRIDE code[29] for a generic WT trajectory.

mass is 10 kJ mol^{-1} fs^2, the width of the Gaussian potential is 0.1, and its height is 0.2 kJ. Gaussian functions are added every 300 fs.

3. Results and Discussion

We show in Figure 2 the values of the chosen collective variable during a single trajectory of WT prion and the corresponding secondary structure evolution in the region of the PrP^C β-sheet. These data confirm that we can sample conformational states with a different amount of local β-structure by forcing the system to explore all the possible S values in the allowed range. These go from $S \simeq 4$, corresponding to a tightly bound three-residue antiparallel β-sheet, to $S = 0.1$ which implies a complete absence of β-structure. It is important to stress that the effective time span of the metadynamics simulation (e.g., 1.8 ns in Figure 2) does not correspond to a "real" time scale, and it is only a measure of the computational effort. In fact, the kinetics of the system is modified by the history-dependent biasing potential so that accessible Gibbs states are sampled more rapidly than in conventional MD. Indeed, in our previous study, a complete breakup was never observed in 16 standard MD simulations of mouse PrP in water for an aggregated simulation time of 28.8 ns.[17] The metadynamics on the other hand was able in only 1.8 ns worth of simulation to explore several disruptions and reformations of the β-sheet. Furthermore by inspecting Figure 2 we note that there is a strict correlation between the canonical secondary structure assignment and the corresponding S values for all the sampled configurations. To show quantitatively this correspondence, we evaluated the value of the S coordinate as a function of the instantaneous length of the antiparallel β-sheet, averaged over all 12 runs of the mutant and of the WT prion. The S value corresponding to a β-sheet length of 0, 1, 2, and 3 residues is 0.2, 1.5, 1.7, and 2.6, respectively.

In Table 1 we report the average α-carbons root-mean-square displacements (RMSD) from the experimental structure for the WT PrP^C and its D187N mutant. As expected the overall RMSDs coming from metadynamics are slightly higher than RMSDs obtained from standard MD.[17,16] In particular, the largest deviations are localized in the sequence containing the β-sheet and helix 1 (124−171). The RMSD data also show a remarkable insensitivity in the 172−226 sequence, including

Table 1. α-Carbon RMSDs and Relative Standard Deviations Calculated for the WT PrP^C and Its D178N Mutant^a

PrP^C sequence	WT	D178N
124−226	2.8 ± 0.3	2.7 ± 0.4
124−171	3.1 ± 0.4	2.8 ± 0.6
172−226	2.1 ± 0.2	2.1 ± 0.5

^{a} Three different PrP sequences have been considered: the 124−226 sequence corresponds to the whole domain; the 124−171 sequence corresponds to the two β-strands and to α-helix 1; the 172−226 sequence corresponds to the α-helices 2 and 3.
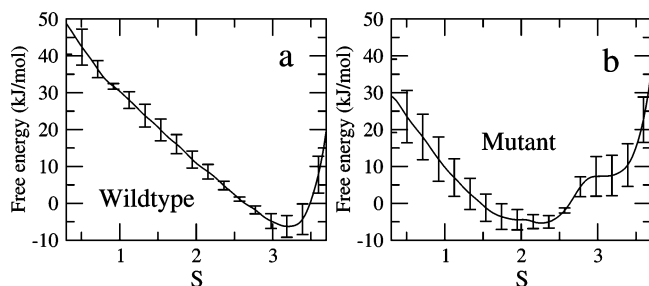

Figure 3. Free energy as a function of *S* for the WT (a) and the D178N mutant (b). The FESs are both arbitrarily set to zero at *S* = 2.63, which corresponds, on average, to a three-residue β-sheet. The reported functions may therefore be seen as the free energy difference between a general state along the *S* coordinate and a three-residue β-sheet. The error bars represent the uncertainties of these free energy differences.

helix 2 and 3, to conformational changes in the 124−171 flanking sequence. The insensitivity of the 172−226 sequence to changes in the 124−171 sequence agrees well with the observed pattern of its contact map[19] with few contacts involving residues outside the helix 2 and helix 3 region. This suggests that either 124−171 or 172−226 PrP^C regions may misfold independently if the reaction is initiated along the *S* coordinate. In this respect it has been recently found that helix 2 and helix 3 are frustrated indicating a possible role of these structural elements in the formation of intermediates for the misfolded isoform.[30,19]

In Figure 3 we compare the free energy dependence on the *S* coordinate of the WT PrP^C and of its D178N mutant. The minimum of the FES of the WT PrP^C (*S* = 3.14) corresponds to a tightly bound three-residue-long β-sheet. This is in agreement with previous MD simulations[13,18,31] on mouse PrP^C, and it is consistent with NMR data.[32,33] In the experimental mouse PrP^C structure (PDB code: 1AG2), the β-sheet can indeed be considered either four residues long on the basis of NOE signals and amide-proton exchange factors[32] or two residues long on the basis of standard secondary structure analysis codes (DSSP,[34] STRIDE[29]). In the D178N mutant the β-sheet turned out to be markedly less stable. This can be seen in the much shallower minimum of the FES which is shifted to lower *S* values. The results reported in Figure 3 are compatible with previous conventional MD studies. In fact a weakening of the β-sheet in the D178N mutant with respect to the WT prion was observed by Sekijima et al.[16] as well as in some of the

independent MD simulations of D178N in water reported in our previous study.[17]

As mentioned in the Introduction, Asp178 interacts strongly via H-bonds with the side chains of the residues Arg164 and Tyr128 in the native form.[33] As these latter residues are part of, or immediately adjacent to, the β-strands, the cluster Arg164, Tyr128, Asp178 may indeed play an important role in stabilizing the β-structure itself. In particular, damage in the H-bonding network, due to the replacement Asp178 → Asn, could account for the observed diminished stability of the antiparallel β-sheet in the D178N mutant.

A measure of the strength of these interactions can be obtained from Figure 4, where the distribution function of the minimum distances between the contacts in the relevant side chain triad is shown. In particular in Figure 4a we report the contact between Tyr128 and Asx178 (Asp178 in the WT or Asn178 in the D178N mutant). The WT distribution function is characterized by a sharp peak corresponding to the H-bond between one Asp178 carboxylic oxygen and the Tyr128 hydroxy hydrogen and by a secondary broader peak due to side chain interactions mediated by bridged water molecules. In the D178N mutant, the distribution function is qualitatively similar to that of the WT, although the main peak is less pronounced and shifted toward large distances, indicating a weaker H-bond. In Figure 4b the distribution functions of the contact between Arg164 and Asx178 are reported. For this specific interaction, the mutant distribution differs remarkably from the WT one. Indeed, in the latter a persistent H-bond tightly holding together Arg164 and Tyr128 is observed, whereas the D178N mutant exhibits only a broad and structureless distribution, indicating a rather loose or negligible interaction between Arg164 and Asn178.

Experimentally it has been observed that in acid pH the mobility of the β-sheet in human PrP^C increases.[35] If we assume that solvent exposed Asp178 could be protonated, this experimental observation appears to confirm the stabilization role of this residue. In light of this, it appears tempting to establish a connection between the loss of the salt bridge in the D178N mutant and the weakening of the β-sheet. This would lend credit to the theories according to which PrP^C misfolding proceeds, at some stage, via the breakup of the antiparallel β-sheet, thereby implying a not necessarily antiparallel β-structure in PrP^{Sc} as suggested by Wille et al.[2,3]

To shed further light on this correlation and at the same time clarify the functional role of the salt bridge in preserving the PrP^C fold, we report in Figure 5 the Tyr128-Asx178 and Arg164-Asx178 interresidue distances as a function of the *S* coordinate. In the WT (Figure 5a) lower *S* values correspond to stretched inter-residual distances. In particular, the Tyr128-Asp178 average distance appears to be rather insensitive to the *S* coordinate in the range 1 < *S* < 4, while it increases rapidly at lower values of *S* when the β-sheet is broken. On the other side, the Asp178-Arg164 interaction decreases more steadily with decreasing *S*. In the D178N mutant simulations (Figure 5b), the interresidue distances are not correlated to the *S* values and, therefore, not to the β-sheet stability.

These data suggest the following picture: in WT PrP^C the interactions between Asp178-Arg164 and Asp178-Tyr128 provide a structural constraint that holds the β-strands together.

(29) Frishman, D. based protein secondary structure assignment. 1995 Dec; 23-(4): 566−79., P. A. K. *Proteins* **1995**, *23*, 566−579.
(30) Thirumalai, D.; Klimov, D. K.; Dima, R. I. *Curr. Opin. Struct. Biol.* **2003**, *13*, 146−150.
(31) Parchment, O. G.; Essex, J. W. *Proteins* **2000**, *38*, 327−340.
(32) Riek, R.; Hornemann, S.; Wider, G.; Billeter, M.; Glockshuber, R.; Wüthrich, K. *Nature* **1996**, *382*, 180−182.
(33) Riek, R.; Wider, G.; Billeter, M.; Hornemann, S.; Glockshuber, R.; Wüthrich, K. *Proc. Natl. Acad. Sci. U.S.A.* **1998**, *95*, 11667−11672.
(34) Kabsch, W.; Sander, C. *Biopolymers* **1983**, *22*, 2577−2637.

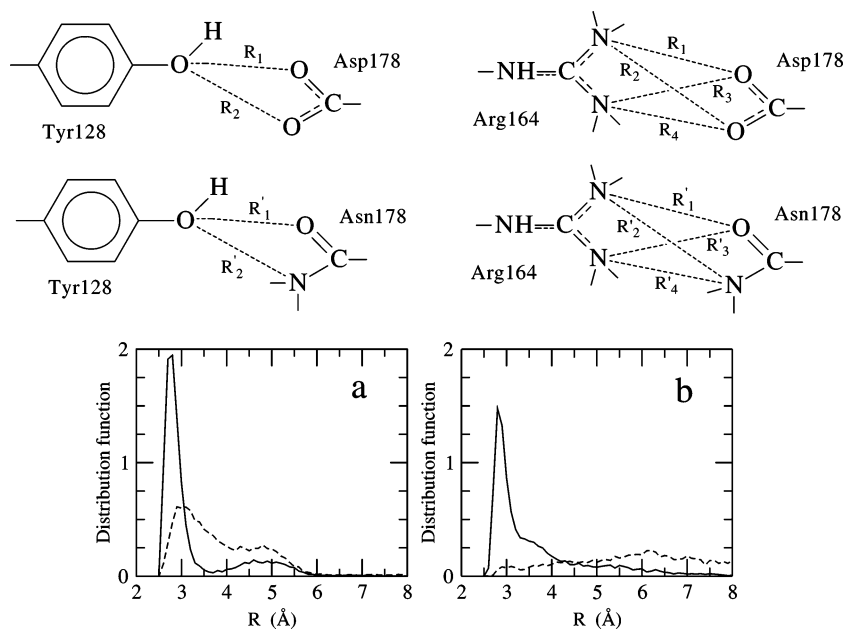(35) Calzolai, L.; Zahn, R. *J. Biol. Chem.* **2003**, *278*, 35592−35596.

Figure 4. (a) Distribution function of the minimum distance between the Tyr128-Asp178 residues (i.e., $\min(R_1, R_2)$) of the WT (solid line) and the Tyr128-Asn178 residues (i.e., $\min(R'_1, R'_2)$) of the D178N mutant (dashed line). (b) Distribution function of the minimum distance between the Arg164-Asp178 residues (i.e., $\min(R_1, R_2, R_3, R_4)$) of the WT (solid line) and the Arg164-Asn178 residues (i.e., $\min(R'_1, R'_2, R'_3, R'_4)$) of the D178N mutant (dashed line).
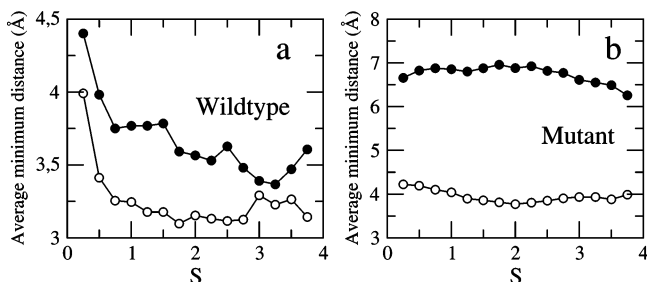

Figure 5. (a) Average minimum distance between the Tyr128-Asp178 residues (○) and the Arg164-Asp178 residues (●) of the WT as a function of the S coordinate. (b) Average minimum distance between the Tyr128-Asn178 residues (○) and the Arg164-Asn178 residues (●) of the D178N mutant as a function of the S coordinate. See Figure 4 for the definition of minimum distance between residues.

The abrupt change in the behavior of the distance at low S values in the WT indicates in fact that the 3-fold interaction Asp178-Arg164-Tyr128 is very likely to provide the thermodynamic barrier for the unzipping of the two β-strands when the appropriate fluctuation occurs. As suggested by the sharp increases at low S values (see Figure 5a), this barrier for the WT structure must be located near or at the zero of the S coordinate. In the D178N mutant, this mechanism, as demonstrated in Figures 4 and 5, is no longer active and the β-sheet is more easily broken and reformed.

4. Conclusions

In the present study we have developed a reaction coordinate to investigate the disruption/growth of the PrP^C antiparallel β-sheet and performed multiple metadynamics simulations for evaluating the free energy difference of this process for the wild-type PrP^C and its D178N mutant. The resulting free energy profiles along the β-sheet coordinate clearly indicate that the antiparallel β-structure is significantly weaker in the pathogenic D178N mutant than in wild-type PrP^C. The destabilization of the PrP^C structure in this region is found to be strongly correlated to the weakening of the hydrogen bonding network involving

residues 164, 128, 178 caused by the replacement of Asp178 by an Asn residue. In fact in wild-type PrP^C the triad 164, 128, 178 appears to hold the two β-strands together even when intrasheet H-bonds are occasionally broken, thereby inhibiting the complete β-sheet breakup and fold destabilization.

As recently reported, mild variation of the natural thermodynamic conditions of PrP^C may easily induce the formation in vitro of PrP^{Sc}-like structures,[12,36-38] leading to the conclusion that PrP^{Sc} is quite probably the thermodynamically stable isoform of the prion sequence[12] and that a high activation energy barrier, or possibly multiple activation energy barriers, renders the transition very slow. In this respect, the observation in the present study that the pathogenic D178N mutation weakens rather than strengthens the PrP^C β-sheet has the following implications:

(i) Past standard MD studies have interpreted occasional elongations of the antiparallel PrP^C β-sheet in pathogenic conditions as a first step toward a misfolded isoform rich in the antiparallel β-structure.[6,7] Our metadynamics simulations, on the other hand, indicate that PrP^C is likely to undergo disruption rather than growth in the initial stage of the PrP^C → PrP^{Sc} conversion. This hypothesis is in agreement with recent electron microscopy studies pointing to a parallel β-fold for PrP^{Sc}.[2,3]

(ii) The β-sheet breaking in PrP^C is likely to be the *first* barrier in PrP^C → PrP^{Sc} conversion. The triad Tyr128, Asp178, and Arg164 contributes to this barrier and provides a safety mechanism against β-strands unzipping, thus preserving PrP^C fold. In the D178N mutant this mechanism is severely weakened, allowing the β-strands to unzip with higher probability. A similar effect was also observed experimentally in a different pathogenic condition. NMR experiments on human PrP^{C35} indicated, in fact,

(36) Hornemann, S.; Glockshuber, R. *Proc. Natl. Acad. Sci. U.S.A.* **1998**, *95*, 6010−6014.
(37) Swietnicki, W.; Morillas, M.; Chen, S. G.; Gambetti, P.; Surewicz, W. K. *Biochemistry* **2000**, *39*, 424−431.
(38) Zou, W. Q.; Cashman, N. R. *J. Biol. Chem.* **2002**, *277*, 43942−43947.

that acid pH enhances structural mobility in the region of the second β-strand.

The above statement lends credit to the hypothesis that places the β-rich part of the PrP^{Sc} monomer in the $103-172$ segment encompassing helix 1 and the two bracketing β-strands, as proposed recently.[2,3] In this framework, the observed and surprising stability of helix 1[19,17,39] in different thermodynamic conditions[39] could be rationalized as follows: the inherent stability of this secondary structural element (that is largely independent of PrP flanking sequences and that has a high degree of homology across species[39,19]) is the result of the natural selection aimed at providing a *second* and backup energy barrier to be overcome in the PrP^C $\rightarrow$ PrP^{Sc} transition. In this regard, the metadynamics method can be of great help in identifying possible thermodynamic and/or structural conditions that could play a role in overcoming this hypothetical second barrier, making the transition to the misfolded isoform possible. We are currently investigating in this direction.

(39) Ziegler, J.; Sticht, H.; Marx, U. C.; Müller, W.; Rösch, P.; Schwarzinger, S. *J. Biol. Chem.* **2003**, *278*, 50175−50181.